

Hybrid density-functional theory calculations of electronic and optical properties of mercaptocarboxylic acids on ZnO ($10\bar{1}0$) surfaces

Dennis Franke,^{*,†} Michael Lorke,^{*,‡} Th.Frauenheim,^{*,‡} and A. L. Rosa^{*,¶,‡}

[†]*Bremen Center for Computational Materials Science, University of Bremen, Am Fallturm
1, 28359 Bremen, Germany*

[‡]*BCCMS, Universität Bremen, Am Fallturm 1, 28359, Bremen, Germany*

[¶]*Federal University of Goiás, Institute of Physics, Campus Samambaia, 74690-900,
Goiânia, Goiás, Brazil*

E-mail: defra@uni-bremen.de; mlorke@uni-bremen.de; frauenheim@bccms.uni-bremen.de;
andreialuisa@ufg.br

Abstract

In this work we investigate the electronic properties of mercaptocarboxylic acids with several carbon chain lengths adsorbed on ZnO-(10-10) surfaces via density functional theory calculations using semi-local and hybrid exchange-correlation functionals. Amongst the investigated structures, we identify the monodentate adsorption mode to be stable. Moreover, this mode introduces optically active states in the ZnO gap, is further confirmed by the calculation of the dielectric function at PBE0 and TD-PBE0 levels. One interesting finding is that adsorption mode and the dielectric properties of the hybrid system are both rather insensitive to the chain length, since the acceptor

molecular state is very localized on the sulphur atom. This indicates that even small molecules can be used to stabilize ZnO surface and to enhance its functionality for opto-electronic applications.

Introduction

Hybrid nanostructures made of organic and inorganic materials are of great interest for applications in electronic and optoelectronics devices. ZnO is a semiconductor and a low-cost material with a wide band gap of 3.3 eV, high electron mobility, and high absorbance in the UV range.¹ Besides, ZnO can be synthesized in several nanostructure shapes. ZnO nanowires are of particular interest for electronic transport in one-dimension.² Because of the large surface-to-volume ratio of ZnO nanowires, their optical and electrical properties can be efficiently tailored by surface functionalization. On the other hand, zero dimensional semiconductor nanostructures such as colloidal quantum dots exhibit exceptional optical and electronic properties and photo-stability. These nanostructures have a size-dependent band gap which allows efficient absorption across the broad solar spectrum.³⁻⁵ Recently it has been proposed that surface functionalization of ZnO nanowires using ligand-capped quantum dots lead to hybrid solar cells with high absorption in a wide spectral range.^{6,7} In such hybrid systems, functional groups are attached on both quantum dot and nanowire surfaces.

Ab initio density-functional theory calculations of several small functional groups on ZnO (10 $\bar{1}$ 0) surfaces have been pursued.⁸⁻¹³ In our previous work, we have shown that -SH groups form strong covalent bonds on ZnO (10 $\bar{1}$ 0) surfaces with a monodentate adsorption mode.^{12,14} Indeed thiols have been investigated experimentally and found to bind strongly to ZnO non-polar surfaces. In particular, molecules with long CH₂ chains are observed to be stable.^{15,16}

In this paper we have investigated mercaptocarboxylic acids (MPA)-derived molecules SH - (CH₂)_n - COOH, (n = 1,2,3,7) on ZnO (10 $\bar{1}$ 0) surfaces. Monodentate adsorption

mode is found to be stable and introduces intragap states which are responsible for changes in the electronic and optical properties of ZnO. Furthermore, adsorption modes and optical properties of the hybrid interfaces are not sensitive to the carbon chain length, which suggests that even small molecules can be used to stabilize and modify the ZnO surface properties.

Computational Details

The calculations were performed using density functional theory (DFT) as implemented in the Vienna ab initio simulation package (VASP).^{17,18} The projected augmented wave method has been used.^{19,20} The atomic structures were optimized using the PBE functional.²¹ To get better description of the electronic structure, the PBE0 hybrid functional²² has been employed. This functional can reproduce reasonably well the ZnO band gap.²³ A plane wave basis with an energy cutoff of $E_{\text{cut}} = 400$ eV and a $(1 \times 4 \times 4)$ Monkhorst-Pack \mathbf{k} -point sampling has been used. The dielectric function has been calculated in the independent particle approximation with the PBE0 functional (IPA-PBE0). Additionally time-dependent density-functional theory with the PBE0 functional (TD-PBE0) has been used to include excitonic effects. In this case, only the Γ point has been considered. The surfaces have been modeled using the slab approach with a (3×2) surface supercell containing 96 atoms (48 ZnO units) units and a single MPA molecule.

Results

We have explored several geometries for the MPA molecules on the ZnO $(10\bar{1}0)$ surfaces. The ground-state geometries for SH-(CH₂)_n-COOH on ZnO are shown in Fig. 1 (a)-(d) for both monodentate and Fig. 1 (e)-(h) bidentate binding modes. These geometries were optimized at the PBE level, as explained in our previous calculations.^{12,14} The preferred adsorption mode is the monodentate mode with the molecule sitting at top sites. This mode is more stable against bridge and hollow positions. In both cases the MPA molecules adsorb in

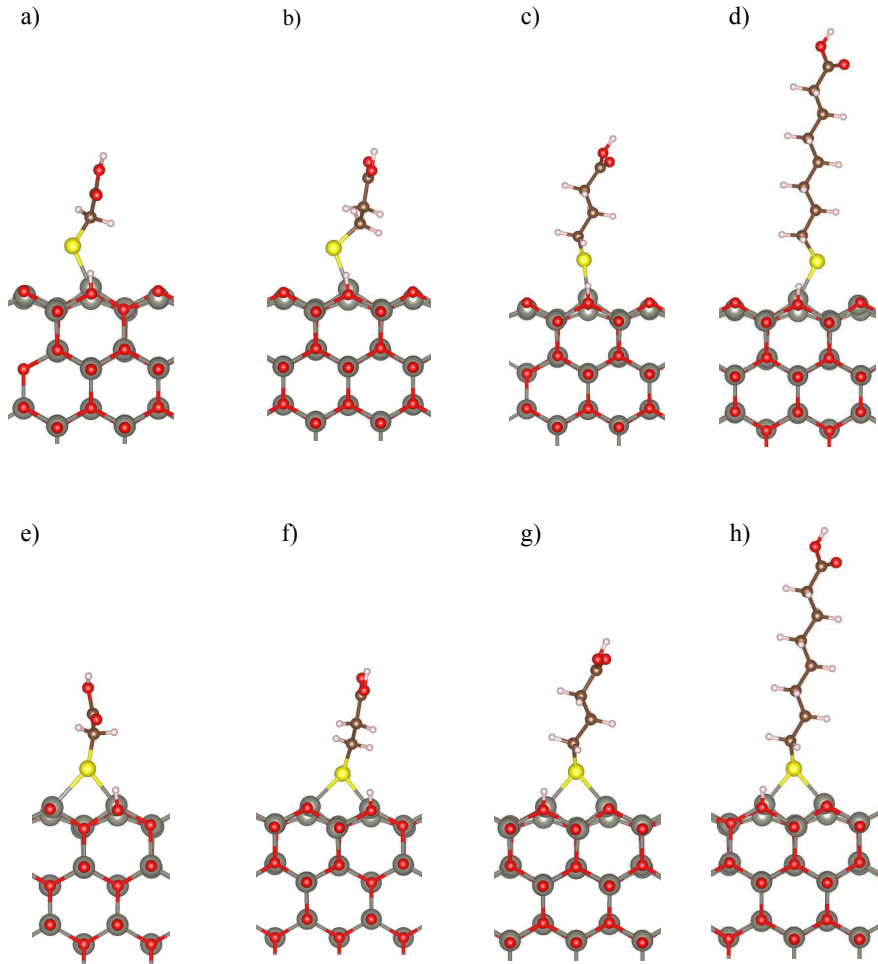


Figure 1: Optimized structures with PBE for the $(10\bar{1}0)$ ZnO surface functionalized with MPA with a monodentate binding mode a) $\text{SH}-(\text{CH}_2)_n$, a) $n=1$, b) $n=2$, c) $n=3$, d) $n=7$ and bidentate mode e) $n=1$, f) $n=2$, g) $n=3$ and h) $n=7$.

a dissociative manner. Table 1 shows the bond lengths between the sulphur atom of the molecule and the outermost zinc atom of the ZnO surface $d_{\text{Zn-S}}(\text{\AA})$, the relaxation of the zinc atom which is bonded to the sulphur atom relative to the zinc atoms of the ZnO surface Δz , the energy difference ΔE between the monodentate and bidentate configurations and the adsorption energy of the MPA molecules $E_{\text{ads}}(\text{eV})$ on the ZnO surface. The monodentate mode is the most stable configuration for all investigated carbon chain lengths, diminishing as the chain length increases. The molecules sit relatively upright on the surface. The Zn-S bond length and the buckling remains almost constant for all the structures, indicating that the interaction of the molecules with the surface is strong (around 1 eV), as it can be

seen from the adsorption energies in Table 1. In this work we have consider a low coverage regime. In our case we have investigated a coverage of 1 molecule/nm², but densities up to 4.6 molecules/nm² have been reported.¹⁶ Larger coverage values need to be investigated in order to see whether the monodentate mode remains stable against the bidentate mode.

Table 1: Outward relaxation of the surface zinc atom Δz , Zn-S bond length $d_{\text{Zn-S}}$, energy difference ΔE between the monodentate and bidentate modes and adsorption energy for the monodentate mode $E_{\text{ads}} = E_{\text{tot}}^{\text{MPA/ZnO}} - E_{\text{tot}}^{\text{bare surf}} - E_{\text{tot}}^{\text{MPA}}$ of SH-(CH₂)_n-COOH (n=1,2,3,7) molecules on ZnO (10 $\bar{1}$ 0) surfaces. $E_{\text{tot}}^{\text{MPA/ZnO}}$, $E_{\text{tot}}^{\text{bare surf}}$ and $E_{\text{tot}}^{\text{MPA}}$ are the total energy of the hybrid MPA/ZnO interface, of the bare ZnO (10 $\bar{1}$ 0) surface and of the MPA-derived molecules with different chain lengths, respectively.

| chain length n | $\Delta z(\text{\AA})$ | $d_{\text{Zn-S}}(\text{\AA})$ | $\Delta E(\text{eV})$ | $E_{\text{ads}}(\text{eV})$ |
|------------------|------------------------|-------------------------------|-----------------------|-----------------------------|
| 1 | 0.28 | 2.26 | -2.20 | 1.00 |
| 2 | 0.35 | 2.23 | -1.90 | 1.00 |
| 3 | 0.28 | 2.26 | -1.10 | 1.10 |
| 7 | 0.28 | 2.26 | -0.70 | 1.10 |

The total and projected density-of-states (PDOS) calculated at the PBE0 level are shown in Fig. 2. The eigenvalues have been aligned according to the electrostatic potential of the vacuum region as described in Ref.²⁴ The zero of the energy is set at the highest occupied state of the bare ZnO (10 $\bar{1}$ 0) surface shown in Fig. 2(a) as explained in our previous investigations Ref.^{12,14} For all functionalized structures, intra-gap states are found, as it can be seen in Figs. 2(b)-(e). These states are mainly localized on the sulphur atom and at the first -CH₂ group of the molecule. The difference between the state located at valence band maximum (VBM) and the occupied state inside the gap remains unchanged, confirming that the electronic structure of the hybrid system is dominated by the interaction between atoms close to the surface. In order to provide further information on charge localization, we have calculated the band decomposed partial charge density at the Γ point, as shown in Fig. 2 for SH - (CH₂)₃ - COOH and SH - (CH₂)₇ - COOH molecules. The figures on the left correspond to the highest-minus-one-occupied orbital in SH-(CH₂)₃-COOH (top left) and SH-(CH₂)₇-COOH (top right) on the (10 $\bar{1}$ 0) ZnO surface. The figures on the right corre-

respond to the highest occupied orbital in SH-(CH₂)₃-COOH (top left) and SH-(CH₂)₇-COOH (top right) on the (10 $\bar{1}$ 0) ZnO surface. The corresponding A and B states are indicated in the Figs. 2 (c) and (e). Both molecular states (PDOS shown in green) are clearly dominated by contributions from sulphur-*p* orbitals from the molecules (PDOS shown in red), with small hybridization both with the ZnO surface and the neighboring CH₂ groups. This feature is found for all investigated structures. The band decomposed partial charge for the MPA molecules with smaller chains (n=1 and n=2) show a similar behavior (see Fig. S1 in Supporting Information). This indicates that MPA molecules with -SH groups attached to the ZnO surface, the -CH₂ groups plays a minor role in the charge transfer process and consequently on the electronic structure of the system.

The presence of the intra-gap states raises the question whether these systems can be used to enhance or modify the optoelectronic properties of the ZnO non-polar surfaces. Therefore we have calculated the dielectric function of the bare and functionalized surfaces in the IPA.²⁵ The ϵ_{\perp} component shown in Fig. 3 (a) corresponds to the propagation of the electromagnetic field perpendicular to the surface while ϵ_{\parallel} in Fig. 3 (b) corresponds to the field being parallel to the surface. We find that in both cases the intra-gap states are optically active. Especially for ϵ_{\perp} a peak around 2.3 eV is clearly visible for larger chains, stemming from transitions between the molecular state B and the ZnO conduction band. Additionally, the spectra reveal a shoulder at the low energetic side of the band-to-band transition, that corresponds to a transition between the state A and the ZnO conduction band. For smaller carbon chain lengths such as for n=2, only the latter is found. This is because the charge is less localized across the surface and extends to the functional group -COOH located at the upper end of the molecule. Therefore, depending on the intended charge localization one can choose the proper carbon chain length to be used.

The discussion above does not include the presence of excitonic effects. However, more accurate predictions of materials for optoelectronic applications requires the inclusion of the electron-hole pair, which can be achieved using theoretical methods at different approxi-

mations, such as GW + Bethe-Salpeter equation (BSE) or TD-DFT.²⁶ Previous theoretical investigations reported excitation energies for catechol and dopamine interactions with TiO₂ surfaces using TD-DFT.²⁷ Therefore, in addition to the PBE0 calculations for the dielectric function, we have performed TD-DFT calculations²⁶ so that occupied and empty one-electron states are calculated using the PBE0 functional. As discussed in Ref.,²⁶ this approach should lead to excitation spectra which are improved compared to the IPA-PBE0 approach and equivalent to the solution of the BSE equation. In this manner, excitonic effects can be captured to a certain extent. The dielectric function is then obtained by solving the Casida's equation.²⁸ Our results for the MPA with $n = 3$ are shown in Fig. 3 (a) for ϵ_{\perp} and (b) for ϵ_{\parallel} . Our results show that the inclusion of many-body effects in TD-PBE0 causes a red shift of the spectrum. Further experiments to validate our results are needed. Also, it would be useful to have the absorption spectrum calculated with GW+BSE, but this is still prohibitive due to the high computational costs. Furthermore, we would like to point out that, even though the spectra are calculated here in the IPA, the inclusion of excitonic (ladder) effects is not expected to change the physical picture significantly, as the exciton binding energies between localized molecular states and delocalized conduction band states should be weak due to a small wave function overlap in the corresponding exchange Coulomb matrix elements. Hence, we believe that the absorption due to the presence of -SH groups states around 2.3 eV can be used either to enhance the efficiency of solar cells based on functionalized semiconductor surfaces. Usually, the nanowire growth direction is the [0001] with the non-polar surfaces exposed. Therefore, the field propagation would be most beneficial if it naturally happens along the nanowires surfaces.

Conclusions

We have investigated adsorption of MPA-derived molecules with several carbon chain lengths using semi-local and hybrid functionals. We have identified the monodentate adsorption

mode as the most stable one and have further shown that electronic and optical properties of these hybrid system are not very sensitive to the chain length. The acceptor state located in the band gap is very localized on the molecular orbitals, mainly on the sulphur atom. This indicates that even small molecules can be used to stabilize ZnO non-polar surfaces and tune their dielectric properties. Our results corroborate well with experimental findings which have suggested that this system is promising for optoelectronic applications.

Acknowledgement

The authors acknowledge funding by the DFG research group FOR 1616 “Dynamics and Interactions of Semiconductor Nanowires for Optoelectronics”, CNPq and FAPEG.

Supporting Information Available

The following files are available free of charge.

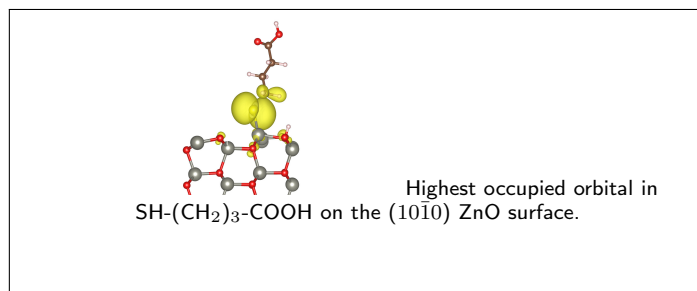
References

- (1) Kolodziejczak-Radzimska, A.; Jesionowski, T. *Materials* **2014**, *7*, 2833.
- (2) Wang, Z.; Song, J. *Science* **2006**, *312*, 242.
- (3) Yang, Z.; Fan, J. Z.; Proppe, A. H.; de Arquer, F. P. G.; Rossouw, D.; Voznyy, O.; X, L.; Liu, M.; Walters, G.; Quintero-Bermudez, R.; Sun, B.; Hoogland, S.; and S. O. Kelley, G. A. B.; Sargent, E. H. *Nat. Comm.* **2017**, *8*, 1325.
- (4) Sargent, E. H. *Nat. Photon.* **2012**, *6*, 133.
- (5) Semonin, O. E.; M.Luther, J.; C.Beard, M. *Materials Today* **2012**, *15*, 508.

- (6) Leschkies, K. S.; Divakar, R.; Basu, J.; Enache-Pommer, E.; Boercker, J. E.; Carter, C. B.; Kortshagen, U. R.; Norris, D. J.; Aydil, E. S. *Nano Lett.* **2007**, 1793.
- (7) Bley, S.; Diez, M.; Albrecht, F.; Resch, S.; Waldvogel, S. R.; Menzel, A.; Zacharias, M.; Gutowski, J.; Voss, T. *J. Phys. Chem. C* **2015**, 119, 15627.
- (8) Bahers, T. L.; Pauporté, T.; Labat, F.; Ciofini, I. *Langmuir* **2011**, 27, 3442.
- (9) Kiss, J.; Langenberg, D.; Silber, D.; Traeger, F.; Jin, L.; Qiu, H.; Wang, Y.; Meyer, B.; Wöll, C. *J. Phys. Chem. A* **2011**, 115, 7180.
- (10) Calzolari, A.; Ruini, A.; Catellani, A. *J. Am. Chem. Soc.* **2011**, 133, 5893.
- (11) Moreira, N. H.; Rosa, A. L.; Frauenheim, T. *Appl. Phys. Lett.* **2009**, 94, 193109.
- (12) Moreira, N. H.; Dominguez, A.; Frauenheim, T.; da Rosa, A. L. *Phys. Chem. Chem. Phys.* **2012**, 14, 15445.
- (13) Shi, X. Q.; Xu, H.; Hove, M. V.; Moreira, N.; Rosa, A.; Frauenheim, T. *Surf. Sci.* **2012**, 606, 289.
- (14) Dominguez, A.; Lorke, M.; Schoenhalz, A. L.; Rosa, A. L.; Frauenheim, T.; Rocha, A. R.; Dalpian, G. M. *J. Appl. Phys.* **2014**, 115, 203720.
- (15) R. E. Ruther, R. F.; Huhn, A. M.; Gomez-Zayas, J.; Hamers, R. J. *Langmuir* **2011**, 27, 10604.
- (16) Chen, J.; Ruther, R. E.; Tan, Y.; Bishop, L. M.; Hamers, R. J. *Langmuir* **2012**, 28, 10437.
- (17) Kresse, G.; Furthmüller, J. *Comput. Mat. Sci.* **1996**, 6, 15.
- (18) Kresse, G.; Furthmüller, J. *Phys. Rev. B* **1996**, 54, 11169.
- (19) Kresse, G.; Joubert, D. *Phys. Rev. B* **1999**, 59, 1758.

- (20) Bloechl, P. *Phys. Rev. B* **1994**, *50*, 17953.
- (21) Perdew, J. P.; Burke, K.; Ernzerhof, M. *Phys. Rev. Lett* **1996**, *77*, 3865–3868.
- (22) Adamo, C.; Barone, V. *J. Chem. Phys.* **1999**, *110*, 6158.
- (23) *CRC Handbook of Chemistry and Physics*, 58th ed.; 1977.
- (24) Alkauskas, A.; Pasquarello, A. *Phys. Rev. B* **2011**, *84*, 125206.
- (25) Gajdos, M.; Hummer, K.; Kresse, G.; Furthmüller, J.; Bechstedt, F. *Phys. Rev. B* **2006**, *73*, 045112.
- (26) Onida, G.; Reining, L.; Rubio, A. *Rev. Mod. Phys.* **2002**, *601*, 2002.
- (27) Luppi, E.; Urdaneta, I.; Calatayud, M. *J. Phys. Chem. C* **2016**, *120*, 5115.
- (28) Casida, M. E. *Recent Advances in Density Functional Methods*; World Scientific, Singapore, edited by D. P. Chong, 1995; Vol. 1.

Graphical TOC Entry



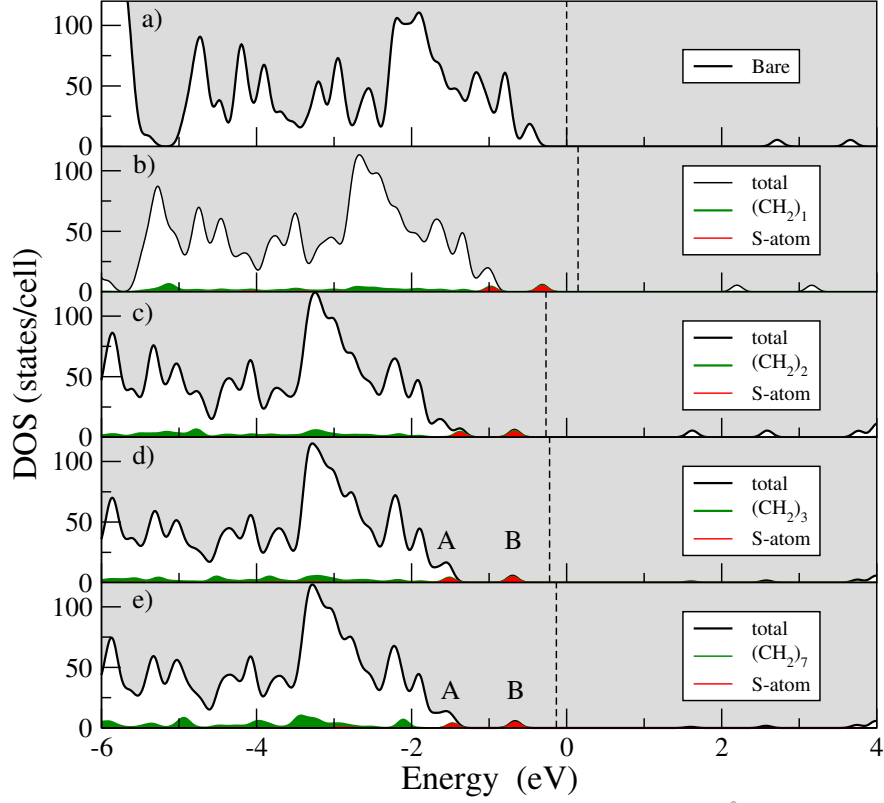


Figure 2: (a)-(e) Total and projected DOS for the bare and modified surfaces with MPA in a monodentate binding mode. The black and green lines represent the total DOS and its projection onto molecular states, respectively. The Fermi energy is denoted by dashed lines. The figures below the DOS show the band decomposed charge density at the Γ point. The figures on the left correspond to the highest-minus-one-occupied orbital in SH-(CH₂)₃-COOH and SH-(CH₂)₇-COOH on the ZnO surface. The figures on the right correspond to the highest occupied orbital in SH-(CH₂)₃-COOH and SH-(CH₂)₇-COOH on (10 $\bar{1}$ 0) ZnO surface. The A and B states are indicated in the DOS (c) and (e).

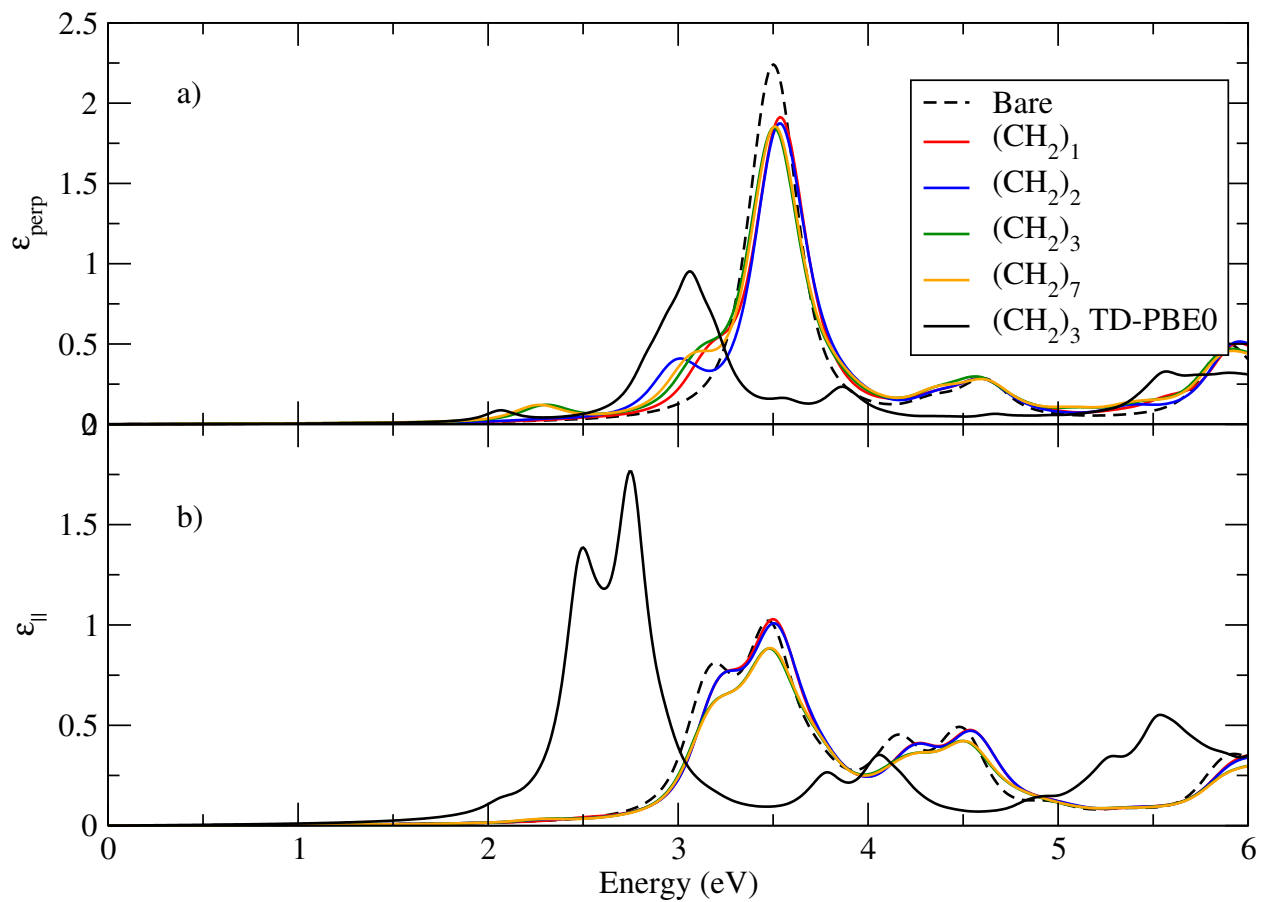


Figure 3: Dielectric function for the bare and modified surfaces with a monodentate binding mode, shown are ϵ_{\perp} (a) and ϵ_{\parallel} (b).